paper 4

by Retno Supriyanti

Submission date: 21-Mar-2023 11:31PM (UTC+0700)
Submission ID: 2042771058
File name: 15142-48819-1-PB-2.pdf (808.85K)
Word count: 6029
Character count: 31962

TELKOMNIKA Telecommunication, Computing, Electronics and Control
Vol. 19, No. 1, February 2021, pp. 63~72
ISSN: 1693-6930, accredited First Grade by Kemenristekdikti, Decree No: 21/E/KPT/2018
DOI: 10.12928/TELKOMNIKA.v19i1.15142

Coronal slice segmentation using a watershed method for early identification of people with Alzheimer's

Retno Supriyanti[1], Anugerah Kevin Marchel[2], Yogi Ramadhani[3], Haris Budi Widodo[4]
[1,2,3]Electrical Engineering Department, Jenderal Soedirman University, Purwokerto, Indonesia
[4]Medical Faculty, Jenderal Soedirman University, Purwokerto, Indonesia

Article Info

Article history:

Received Jan 2, 2020
Revised May 4, 2020
Accepted Sep 5, 2020

Keywords:

Alzheimer
Clinical dementia rating
Hippocampus
Ventricle
Watershed segmentation

ABSTRACT

One physical sign of a person who has Alzheimer's is the diminution of the area of the hippocampus and ventricles. A good quality magnetic resonance imaging (MRI) will provide a high-quality image so that the doctor will quickly analyze the abnormalities of the hippocampus and ventricle area. However, for low-quality MRI, this is difficult to do. This condition will be a significant problem for some regions in developing countries including Indonesia, where many hospitals have only low-quality MRI, and many hospitals do not have them at all. The primary purpose of this research is to develop simple tools to analyze morphological characteristics in Alzheimer's patients. In this paper, we focus only on coronal slice analysis. We will use watershed method segmentation, because of this method able to segment the boundaries automatically, so that parts of the hippocampus and ventricles can be identified in an MRI image. Analysis of morphological characteristics is also classified by age and gender. Then by referring to the value of the clinical dementia rating (CDR), the process of identifying between images with Alzheimer's disease (AD) and healthy models is done based on the morphological analysis that has been done. The results show this method has a better performance compared to the previously work.

Corresponding Author:

Retno Supriyanti
Department of Electrical Engineering
Jenderal Soedirman University
Kampus Blater, Mayjend Sungkono St. KM 5, Blater, Purbalingga 53125, Jawa Tengah, Indonesia
Email: retno_supriyanti@unsoed.ac.id

1. INTRODUCTION

Alzheimer's disease (AD) is a condition that is characterized by a decrease in memory, decreased the ability to think and speak, and changes in behavior in patients due to disorders in the brain that are progressive or slowly (AD) [1]. Currently, this disease is one of the most feared diseases, because this disease is a major disaster that occurs in patients and their families, where the experience of patients who experience it is an endless end until death arrives. AD diagnosis can be made by knowing other forms of dementia, but the determination can only be made after post-mortem studies of brain tissue. This post-mortem study can be done using magnetic resonance imaging (MRI). MRI examination aims to determine the morphological characteristics (location, size, shape, extension, and others of pathological conditions). These objectives can be obtained by assessing one or a combination of axial, sagittal, coronal or oblique cross-sectional images depending on the location of the organ and possible pathology. Image processing is a process of processing an image analysis that aims to improve the quality of the image so can be interpreted by humans or machines (in

this case computers) easily [2]. Currently, many image processing applications are also widely applied in many ways, one of which is the field of medical imaging.

Clinical dementia rating (CDR) is a numerical scale used to measure the severity of symptoms of dementia based on the stage. CDR uses six cognitive and functional domains of performance to identify possible cognitive impairments, namely: memory, orientation, assessment and problem solving, community needs, home & hobbies, and personal care. There are 5 levels of dementia based on the CDR values, namely: 0 (normal), 0.5 (very mild dementia), 1 (mild dementia), 2 (moderate dementia), 3 (severe dementia) [3]. At present, the severity of Alzheimer's refers to the use of the CDR scale, so that a person can be treated according to the severity.

Currently, much research is discussing MRI image analysis about the identification of Alzheimer's. Zubal [4] in his research developed duplication of 123 ^ I-P-CIT striatal V3 "in the case study of Parkinson's disease and applied it to image processing technology. Yu [5] proposed a method of image quality analysis approach that is modeled as a feature extraction expressed in a particular score value. Iannetti [6] used of a protocol that could be used to quantify mitochondria clearly on human skin. Dai [7] developed a 4D extraction tool for brain analysis specifically for adults to be able to analyze MRI images. He uses a deformable extraction algorithm. Kalavathi [8] in his paper, he reviewed the methods available for overall skull analysis. Landau [9] In his research, he standardized the methodology in the use of amyloid PET for Alzheimer's clinical trials. He compared the retention of the compound B (PiB) pittsburgh super-radiotracer and two of the two amyloid radiotracers soup 18 ^ F (florbetapir and flutemetamol) using two types of population models. Eskildsen [10] he proposed a method for predicting the severity of Alzheimer's at a still low level by measuring cortical thickness in MRI images. Zhang [11] he proposed the Alzheimer's detection method using displacement field (DF) which can classify the brain with an AD and healthy brain. Robitaille [12] presented a new technique called STandardization of Intensity (STI) which was used not only to adjust the histogram of the input image into the standard but also to combine information on spatial network intensity. Liu [13] In his research, he proposed a method of brain image segmentation algorithm that combines deformable forms and informative features. Its primary function is to be able to segment with more considerable anatomical variations. Das [14] proposed a method for testing the suitability of high field intensity–magnetic resonance imaging (HF-MRI) in predicting longitudinal changes by comparing measured atrophy levels throughout the hippocampus area using unbiased deformation-based morphometry (DBM). Verclytte [15] he implemented cortical-based surface projections applied to patients with the early-level AD to improve the quality and visualization of image data. Osadebey [16] proposed a method for extracting image features using grayscale and contrast features. Image quality is estimated by measuring structural similarities between the right binary image pairs. Gray [17] conducted an analysis of the incorporation of cross-sectional and longitudinal multi-region fluorodeoxyglucose-positron emission tomography (FDG-PET) information for classification. Ortiz [18] proposed a method for selecting regions of interest (ROI) in brain MRI images to make a diagnosis using vector quantization techniques and statistical learning in patients with an AD. Khajehnejad [19] proposed a method for diagnosing AD at an early stage by using label propagation of a manifold based on semi-supervised learning. Huang [20] proposed longitudinal measurements of MRI brain images and hierarchical classification methods in the classification of the AD to determine the severity of Alzheimer's.

According to the definition of Alzheimer's, the method of diagnosis and studies described above, it will become a problem that is quite important if the diagnosis will be made in a developing country such as Indonesia. As already known, that the equipment used to detect Alzheimer's disease is one of them is MRI that can visualize the anatomy of the human body, especially in parts of the human brain. Furthermore, the doctor will analyze the results of the MRI image to determine the severity of dementia disease based on the information contained in the database. So it can be said that the results of the diagnosis depend very much on the results of the doctor's analysis. The doctor's analysis also depends on the quality of the existing MRI image. The better the MRI machine, the better the quality of the image produced. However, unfortunately in some images that have decreased in quality, for example, contain noise, the color is too contrasting, less sharp, blurred, and so on. The image with poor quality becomes more difficult to interpret because the information delivered is reduced. It happens a lot in images produced by MRI, especially low-resolution MRI. On the other hand, almost all hospitals in Indonesia, including in the province of Central Java, only have low-resolution MRIs, and the numbers are minimal, only in some hospitals [21]. Muneer [22] Muneer developed an IoT-based health monitoring system that was sufficient to overcome the limitations of health facilities.W hen referring to the problems faced by most hospitals in Indonesia, especially the availability of low-quality MRI machines, a manual analysis will be hazardous and may lead to misdiagnosis. Besides referring to the limitations of human resources, especially neuroscientists [21], a simple and accurate device is needed to automatically analyze the MRI image results, especially in the hippocampus and ventricular regions as the primary support in the diagnosis of Alzheimer type dementia. This research has a goal to develop an automatic, low-cost and straightforward tool for analyzing hippocampus and ventricular characteristics in dementia patients by

optimizing existing MRI images. Wibowo [23] used the gray level co-occurrence matrix in analyzing 3D images in muscles. Widodo [24] applies the support vector machine method in recognizing lung disease. Memon [25] applied the Median filter to remove noise in the microscopic image. Supriyanti [26] implemented the histogram equalization method to normalize input images. However, in this paper, we emphasize the discussion on coronal slice analysis only in exploring the morphological information in it. In our previous research [27], we carried out the process of segmenting the coronal slice using the active contour method. However, the results obtained seem to need to be improved again. So in this experiment, we tried to use the watershed method. We tried using the watershed segmentation method because this method is one of the segmentation methods that are widely used in medical images. This method is known as simple, efficient for complex image segmentation, and can produce a complete division of the image into several regions even though the image quality is not good.

2. RESEARCH METHOD

2.1. Data acquisition

The data used in this experiment is from the OASIS database which is publicly provided in the interest of study and analysis. The baseline data consisted of cross-sectional datasets from aged 18 to 96 years and diagnosed clinically with Alzheimer's with a very mild to moderate category [3, 28-31]. The overall experiments conducted in this paper are shown in Figure 1. Based on Figure 1, the segmentation process is carried out by the watershed method. Firstly, the reading of the digital image of the MRI of the coronal slice brain will be processed. Furthermore, the image that has been read by the system will be changed in gray form, and the brightness is adjusted using contrast stretching. Then the image cropping process to take specific region. Then the cropped image is converted into a binary image. This binary image will be an input image in the watershed segmentation process. After the watershed segmentation object is obtained, the extensive calculation process of the hippocampus and ventricles is carried out in pixel units to determine the severity of Alzheimer's based on the CDR value obtained from the OASIS fact sheet.

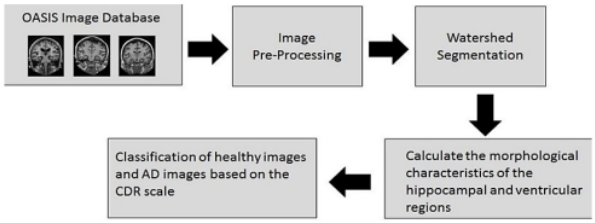

Figure 1. Block diagram of overall experiment

2.2. Image pre-processing

The pre-processing stage is done to get a better image than the initial image. This process is done because to do watershed segmentation, an image with a better level of quality must be obtained concerning lighting. The pre-processing stage includes contrast stretching. It is done to contrast the image more tenuous than before, so that image lighting is better. Contrast stretching is one method of improving image quality. In our previous reserch [32, 33] we did it. Image processing has a higher contrast value so that it can produce new information. It is done by adding or reducing contrast so that the image is sharper than before [2]. It is expected that contrast stretching can produce images that have proper lighting distribution so that the resulting image is visible.

2.3. Watershed segmentation

The segmentation method used is the watershed method for segmenting the hippocampus and ventricular areas. There are several types of watershed segmentation, namely watershed segmentation using distance transformation, using gradients, and using marker-controlled [2]. In this research, we use watershed segmentation using marker-controlled. This type of segmentation is used to control over-segmentation based on the marker concept. What we do is create an internal marker that is inside each desired object and also an external marker that contains the background. These two markers are then used to modify the gradient image. To apply watershed marker-controlled segmentation begins by transforming watershed from gradient images without other processes. Then we calculate the location of all regional minima in the image. The regional

function of minima in gradient images is used to see why watershed functions produce many small catchment basins. The regional minima can also be excessive. Then we calculate the number of "low spots" in the image. Next is an external marker search. The approach is to mark the background with pixel search which is midway between internal markers. To do this is to calculate watershed transformations from the transformation of the marker's internal image distance. After internal and external markers have been obtained, then both are used to modify the gradient image using a procedure called minima imposition. The imposition minima technique modifies the grayscale image so that regional minima occurs only in the marked location.

2.4. Morphological characteristic calculation

The calculation of the area of ventricles and hippocampus is done by calculating the total number of pixels that have a value of 1. The calculated image is binary so that when calculating area it is enough to calculate the number of values that exist in the image matrices. The difference between the calculation of the ventricular area and the hippocampus area is only the number of images calculated. If in the ventricular detection system there is only one image calculated, then in the hippocampus detection system there are two images. It is because of the hippocampus detection system of brain MRI images. It is separated between the left viewer and the right viewer. The area values of the left and right hippocampus are searched and added together respectively. The total summation result is the value of the brain's hippocampal MRI image.

2.5. Image classification

In our experiments, the identification stage in addition to calculating the area of the segmented hippocampus object also identified the CDR value of the brain MRI image used. From this CDR value, it can be seen the severity of a person's Alzheimer's. At the image classification stage, we use backpropagation artificial neural networks (ANN). The training data used is the result of the calculation of the hippocampus and ventricular area that has been carried out on all trial images. Then we determine the training target which is the value of the CDR that is the target of identification. The architectural form of the backpropagation ANN used in this study is 1-2-1 which consists of 1 input, two hidden layers, and one output.

3. RESULTS AND ANALYSIS

As explained in the subsection above, that in this pre-processing phase, we use contrast stretching to get a better input image to be processed. A gray-scale image is a matrix arrangement that has intensity values from 0 to 255. These values represent intensity values in specific rows and columns in the image. So that if changes in value are made, the intensity of the image also changes. The contrast stretching algorithm used in the research is shown in (1).

$$s = \begin{cases} \frac{s1}{r1} r, & 0 \le r < r1 \\ s1 + \frac{(r-r1)*(s2-s1)}{(r2-r1)} \\ s2 + \frac{(r-r2)*(255-s2)}{(255-r2)} \end{cases} \quad (1)$$

The points (r1, s1) and points (r2, s2) determine the form of transformation and can be set to determine the level of spread of the gray level of the resulting image. If r1 = s1 and r2 = s2, then the transformation will be in the form of a straight line which means there is no change in the gray level of the image produced. It is generally assumed that r1 ≤ r2 and s1 ≤ s2 so that the function will produce a single value and the value will always rise. In contrast, stretching algorithm that we use, the values of r1, r2, s1, and s2 have been determined so that we do not need to set them manually. However, between the ventricular detection system and hippocampus detection, the values of r1, r2, s1, and s2 are different. This is because, in their need for watershed segmentation processes, both have differences in the level of image intensity. The values of r1, r2, s1, and s2 in the ventricular detection system are 0.24, 0.25, 0.33 and 0.35. While for Hippocampus detection systems are 0.35, 0.37, 0.39, and 0.41. The values of r1, r2, s1, and s2 that have been determined will form a transformation line as shown in Figure 2.

The values of r1, r2, s1, and s2 selected are obtained from the retesting process. After the experiment using seven more sets of values r1, r2, s1, and s2 for ventricular detection systems and 13 more sets of values r1, r2, s1, and s2 for the hippocampus detection system obtained a set of values that had the highest percentage of success and performance high for both systems. The entire image tested, in reality, does not have a 100% success percentage when segmented due to inaccurate contrast stretching. Although the predetermined values of r1, r2, s1, and s2 have the highest success rates among others, they are still not 100% successful. Figure 3 is an example of the results of contrast stretching using the exact values of r1, r2, s1, and s2 and watershed

segmentation results in ventricular detection. While Figure 4 is an example of the results of using the values r1, r2, s1, and s2 in the detection of the hippocampus.

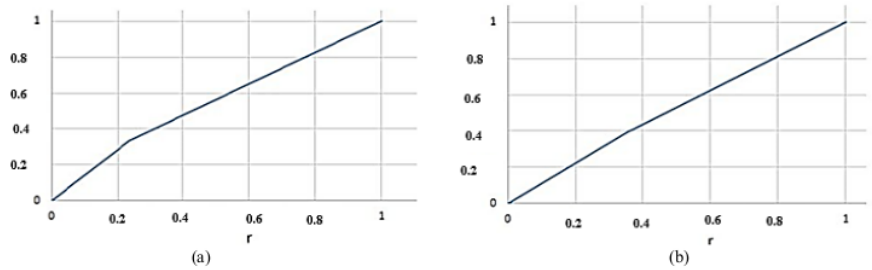

Figure 2. Graph of contrast stretching transformation function of;
(a) ventricular detection system, (b) hippocampus detection system

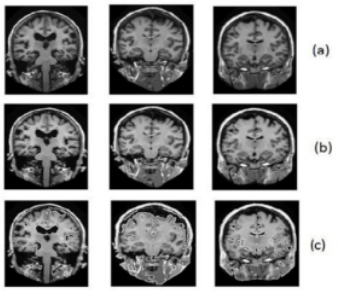

Figure 3. Ventricular detection; (a) original image, (b) contrast stretching results, (c) segmentation results

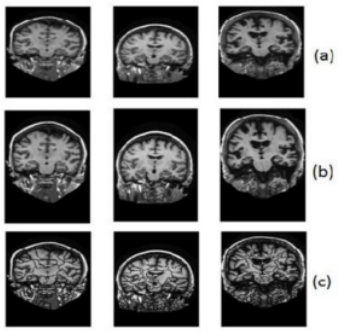

Figure 4. Hippocampus detection; (a) original image, (b) contrast stretching results, (c) segmentation results

Referring to Figure 3 and Figure 4 it can be seen that the image after the contrast stretching process has an even distribution of light compared to the original image. Segmentation used for ventricular detection is a watershed segmentation method using a marker-controlled technique. To use this technique, we look for gradient values from edge detection. The edge detection method used is Sobel edge detection. Then an internal marker search was carried out to be able to process watershed segmentation on distance transformation from the internal marker search results image. The results of the segmentation are used as external markers. This technique results in regional minima occurring only in marked locations. The results of the watershed

segmentation process are displayed in axes. The watershed segmentation process will produce an original image with several watershed lines encircling several objects. This watershed line shows the object that was successfully identified. In the ventricular detection system, the parameters of success of the image segmentation stage are when the watershed line is successfully circling the ventricular object. After seeing a watershed line encircling a ventricular object, cropping is done so that other objects that are also detected by the watershed line are not taken for the next process. The next process is changing the segmented image to a binary image. Figure 5 illustrates the stages of image segmentation in ventricular detection. Referring to Figure 5 it can be seen that the results of watershed segmentation in the form of original images with the addition of a watershed line on some objects have managed to get the desired object, namely ventricles. The ventricular object is surrounded by a watershed line which becomes a reference that the object is successfully segmented.

In the detection system of the hippocampus, the processed image has 2, so there are two orientations, namely in the left viewer and right viewer. The hippocampus detection system is not used single edge detection. To change the technique, we use morphological operations. Then filtering the original image using top-hat transforms and bottom-hat transforms. Then we increase the gap between the existing objects by adding the original image with the top-hat transforms image, then the results of the sum are reduced by the bottom-hat transforms result image. This increase in gap also aims to maximize contrast. Then complementing the image results of this increase in a gap. After this modification, the segmentation process has similarities in detecting ventricles, namely internal marker searches. As in the case of ventricular detection, the detection of the hippocampus will also produce an original image with several watershed lines encircling several objects. However, unlike the watershed line on a ventricular detection system that is white, the watershed line on this system is black. It is because the need for segmentation between ventricular and hippocampal objects is different. Figure 6 shows the results of watershed segmentation in the detection of the hippocampus.

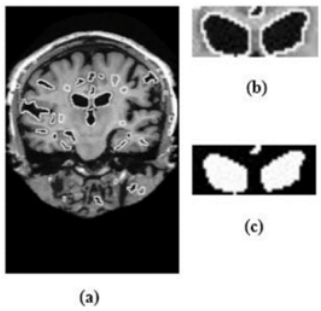

Figure 5. Results of ventricular detection segmentation stages; (a) segmentation results, (b) results of cropping, and (c) form conversion to binary images

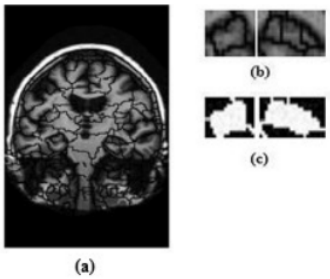

Figure 6. The results of the hippocampus detection segmentation stage; (a) the initial phase of segmentation, (b) the stage of cropping, and (c) the conversion phase to binary

Referring to Figure 6 it can be seen that when the image segmentation stage is executed the hippocampus object is successfully identified on the black colored watershed line. There are also other objects that are also identified. Therefore, there are other watershed lines. To calculate the area of the hippocampus, then we did crop so that other objects do not participate in the area. At the identification stage, the image used is the result of conversion to binary image segmentation results. The binary image then counts the area in pixel size. After obtaining the image area, it can be identified whether the image is an image of a person with Alzheimer's or not based on the CDR level. Figure 7 and Figure 8 shows a graph of the calculation of the average ventricular and hippocampus area based on gender, age and CDR scale.

Referring to Figure 8 information is obtained regarding the average hippocampal area by gender, CDR, and age class. In the average hippocampal area by gender, the average hippocampal area of women is smaller than that of men. The average hippocampal area based on CDR shows that the higher the CDR value, the smaller the hippocampus area. It is by the theory that the higher the CDR value, the smaller the hippocampus. Therefore, the reduction of the hippocampus is one sign of Alzheimer's disease. On the average hippocampus area based on age class, it can be seen that the older a person is, the smaller the hippocampus is. This is following the existing theory that the lower the human age, the higher the likelihood of dementia. Furthermore, after the area of the hippocampus of the brain, MRI image was calculated, the stage of identification of the CDR value was carried out. CDR value is used in determining the level of dementia. Determination of CDR value is done using artificial neural networks.

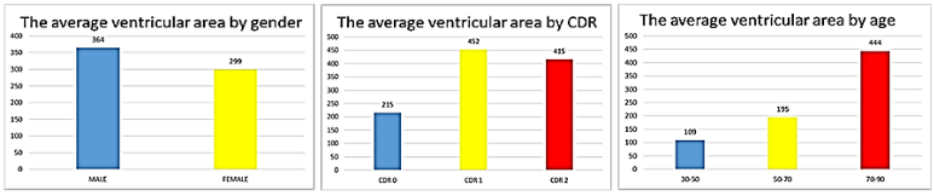

Figure 7. Graph of the average ventricular area by gender, age and scale of CDR

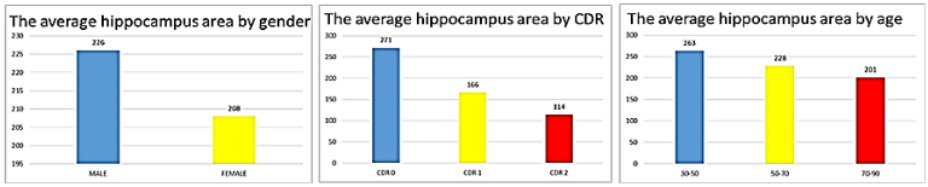

Figure 8. Graph of the average hippocampus area by gender, age and scale of CDR

The architectural form of the backpropagation ANN used in this study is 1-2-1 which consists of 1 input, two hidden layers, and one output. In this experiment, we use the binary sigmoid activation function in the hidden layer and the linear activation function at the output layer. While the training function uses the gradient descent method. The weight value used is random. Table 1 shows the results of identifying CDR values for brain MRI images that were used as test data in this experiment.

Table 1 it can be seen that the process of identifying CDR has satisfactory performance. From 40 test data, the system can recognize CDR values accurately for 39 images. Following are the performance calculation:

$$\frac{39}{40} \times 100\% = 97{,}5\%$$

As we stated in the subsection above, that our previous research tried to use the active contour method to segment the hippocampus and ventricular areas to calculate the area. Comparison of identification results is shown in Table 2.

Table 1. Results of identification of CDR values

NO	ID	MALE/FEMALE	Age	CDR	Identification Result
1	OAS1_0001_MR1	F	74	0	0
2	OAS1_0002_MR1	F	55	0	0
3	OAS1_0011_MR1	F	52	0	0
4	OAS1_0019_MR1	F	89	0	0
5	OAS1_0020_MR1	F	48	0	0
6	OAS1_0026_MR1	F	58	0	0
7	OAS1_0030_MR1	F	65	0	0
8	OAS1_0033_MR1	F	80	0	0
9	OAS1_0044_MR1	F	47	0	0
10	OAS1_0058_MR1	F	46	0	0
11	OAS1_0010_MR1	M	74	0	0
12	OAS1_0018_MR1	M	39	0	0
13	OAS1_0034_MR1	M	51	0	0
14	OAS1_0065_MR1	M	90	0	0
15	OAS1_0069_MR1	M	33	0	0
16	OAS1_0074_MR1	M	43	0	0
17	OAS1_0110_MR1	M	84	0	0
18	OAS1_0114_MR1	M	62	0	0
19	OAS1_0130_MR1	M	68	0	0
20	OAS1_0135_MR1	M	64	0	0
21	OAS1_0035_MR1	F	84	1	1
22	OAS1_0052_MR1	F	78	1	1
23	OAS1_0053_MR1	F	83	1	1
24	OAS1_0056_MR1	F	72	1	1
25	OAS1_0067_MR1	F	71	1	1
26	OAS1_0184_MR1	F	65	1	1
27	OAS1_0269_MR1	F	72	1	1
28	OAS1_0316_MR1	F	72	1	1
29	OAS1_0382_MR1	F	67	1	1
30	OAS1_0031_MR1	M	88	1	1
31	OAS1_0134_MR1	M	80	1	1
32	OAS1_0223_MR1	M	84	1	1
33	OAS1_0268_MR1	M	78	1	1
34	OAS1_0399_MR1	M	78	1	1
35	OAS1_0405_MR1	M	77	1	1
36	OAS1_0424_MR1	M	75	1	1
37	OAS1_0430_MR1	M	71	1	1
38	OAS1_0452_MR1	M	75	1	1
39	OAS1_0308_MR1	F	78	2	2
40	OAS1_0351_MR1	M	86	2	1

Table 2. Performance comparison between segmentation of active contour method and watershed method

No	Method	Performance
1	Active Contour	93.75%
2	Watershed	97.5%

4. CONCLUSION

Contrast values are influencing Segmentation using the watershed method. Watershed line that appears after the watershed segmentation process is run indicates an object that has been successfully segmented by separating the segmentation area using lines. The average hippocampus area of the MRI image of the brain of dementia patients is smaller than that of the MRI image of a healthy person's brain. The average hippocampus area of the MRI image of the human brain over 50 years is smaller than those under 50 years. The results of watershed segmentation of ventricles and hippocampus do not have 100% accuracy or performance regarding detecting the actual shape, but already have a reasonably good accuracy or performance compared to the active contour method we have done before. For further research, it is expected to be able to find the volume of the hippocampus and ventricular by watershed segmentation method so that it can be used as another reference to determine the level of dementia.

ACKNOWLEDGEMENTS

We Thank the Open Access Series of Imaging Studies (OASIS) datasets and in the associated PubMed Central submission: P50 AG05681, P01 AG03991, R01 AG021910, P50 MH071616, U24 RR021382, R01 MH56584. These works are supported by the Directorate of Research and Community Service, Ministry of Research and Technology Indonesia through “Fundamental Resaerch” Scheme

REFERENCES

[1] G. McKhann, D. Drachman, M. Folstein, R. Katzman, D. Price, and E. M. Stadlan, "Clinical diagnosis of Alzheimer's disease: Report of the NINCDS-ADRDA Work Group under the auspices of Department of Health and Human Services Task Force on Alzheimer's Disease," *Neurology*, vol. 34, pp. 939–944, 1984.

[2] Rafael C. Gonzalez and Richard E. Woods, "Digital Image Processing," 3rd edition. New Jersey: *Prentice Hall*, 2008.

[3] J. Morris, "The Clinical Dementia Rating (CDR): current version and scoring rules.," *Neurology*, vol. 43, pp. 2412b-2414b, 1993.

[4] I. G. Zubal, M. Early, O. Yuan, D. Jennings, K. Marek, and J. P. Seibyl, "Optimized, Automated Striatal Uptake Analysis Applied to SPECT Brain Scans of Parkinson's Disease Patients," *J. Nucl. Med.*, vol. 48, no. 6, pp. 857-864, 2007.

[5] S. Yu, S. Wu, L. Wang, F. Jiang, Y. Xie, and L. Li, "A shallow convolutional neural network for blind image sharpness assessment," *PLoS One*, vol. 12, no. 5, pp. 1-17, 2017.

[6] E. F. Iannetti, J. A. M. Smeitink, J. Beyrath, P. H. G. M. Willems, and W. J. H. Koopman, "Multiplexed high-content analysis of mitochondrial morphofunction using live-cell microscopy," *Nat. Protoc.*, vol. 11, no. 9, pp. 1693-1710, 2016.

[7] Y. Dai, Y. Wang, L. Wang, G. Wu, F. Shi, and D. Shen, "aBEAT: A Toolbox for Consistent Analysis of Longitudinal Adult Brain MRI," *PLoS One*, vol. 8, no. 4, 2013.

[8] P. Kalavathi and V. B. S. Prasath, "Methods on Skull Stripping of MRI Head Scan Images—a Review," *J. Digit. Imaging*, vol. 29, no. 3, pp. 365-379, 2016.

[9] S. M. Landau, *et al.*, "Amyloid PET imaging in Alzheimer's disease: A comparison of three radiotracers," *Eur. J. Nucl. Med. Mol. Imaging*, vol. 41, no. 7, pp. 1398-1407, 2014.

[10] S. F. Eskildsen, P. Coupé, D. García-Lorenzo, V. Fonov, J. C. Pruessner, and D. L. Collins, "Prediction of Alzheimer's disease in subjects with mild cognitive impairment from the ADNI cohort using patterns of cortical thinning," *Neuroimage*, vol. 65, pp. 511-521, 2013.

[11] Y. Zhang and S. Wang, "Detection of Alzheimer's disease by displacement field and machine learning," *PeerJ*, vol. 3, 2015.

[12] N. Robitaille, A. Mouiha, B. Crépeault, F. Valdivia, and S. Duchesne, "Tissue-based MRI intensity standardization: Application to multicentric datasets," *Int. J. Biomed. Imaging*, vol. 2012, 2012.

[13] C. Y. Liu, J. E. Iglesias, and Z. Tu, "Deformable templates guided discriminative models for robust 3D brain MRI segmentation," *Neuroinformatics*, vol. 11, no. 4, pp. 447-468, 2013.

[14] S. R. Das, *et al.*, "Measuring longitudinal change in the hippocampal formation from in vivo high-resolution T2-weighted MRI," *Neuroimage*, vol. 60, no. 2, pp. 1266-1279, 2012.

[15] S. Verclytte, R. Lopes, C. Delmaire, J. C. Ferre, F. Pasquier, and X. Leclerc, "Optimization of brain perfusion image quality by cortical surface-based projection of arterial spin labeling maps in early-onset Alzheimer's disease patients," *Eur. Radiol.*, vol. 25, no. 8, pp. 2479-2484, 2015.

[16] M. E. Osadebey, M. Pedersen, D. L. Arnold, and K. E. Wendel-Mitoraj, "Standardized quality metric system for structural brain magnetic resonance images in multi-center neuroimaging study," *BMC Med. Imaging*, vol. 18, no. 1, pp. 1-20, 2018.

[17] K. R. Gray, R. Wolz, R. A. Heckemann, P. Aljabar, A. Hammers, and D. Rueckert, "Multi-region analysis of longitudinal FDG-PET for the classification of Alzheimer's disease," *Neuroimage*, vol. 60, no. 1, pp. 221-229, 2012.

[18] A. Ortiz, J. M. Górriz, J. Ramírez, F. J. Martinez-Murcia, and , Alzheimer's Disease Neuroimaging Initiative, "Automatic {ROI} Selection in Structural Brain {MRI} Using {SOM} {3D} Projection.," *{PLoS} One*, vol. 9, no. 4, 2014.

[19] M. Khajehnejad, F. H. Saatlou, and H. Mohammadzade, "Alzheimer's disease early diagnosis using manifold-based semi-supervised learning," *Brain Sci.*, vol. 7, no. 8, pp. 1-20, 2017.

[20] M. Huang, W. Yang, Q. Feng, and E. All, "Longitudinal measurement and hierarchical classification framework for the prediction of Alzheimer's disease," *Sci. Rep.*, vol. 7, no. November 2016, pp. 1-14, 2017.

[21] Y. Mahendradhata, *et al.*, "The Republic of Indonesia Health System Review," *World Health Organization, Regional Office for South-East Asia*, vol. 7, no. 1, 2017.

[22] A. Muneer, S. M. Fati, and S. Fuddah, "Smart health monitoring system using IoT based smart fitness mirror," *TELKOMNIKA Telecommunication Computing Electronics and Control,* vol. 18, no. 1, pp. 317-331, 2020.

[23] H. Wibowo, E. M. Yuniarno, A. Widayati, and M. H. Purnomo, "Frontalis muscle strength calculation based on 3D image using Gray Level Co-occurrence Matrix (GLCM) and confidence interval," *TELKOMNIKA Telecommunication Computing Electronics and Control,* vol. 16, no. 1, pp. 368-375, 2018.

[24] S. Widodo, R. N. Rohmah, B. Handaga, and L. D. D. Arini, "Lung diseases detection caused by smoking using support vector machine," *TELKOMNIKA Telecommunication Computing Electronics and Control,* vol. 17, no. 3, pp. 1256-1266, 2019.

[25] M. H. Memon, T. J. S. Khanzada, S. Memon, and S. R. Hassan, "Blood image analysis to detect malaria using filtering image edges and classification," *TELKOMNIKA Telecommunication Computing Electronics and Control,* vol. 17, no. 1, pp. 194-201, 2019.

[26] R. Supriyanti, S. A. Priyono, E. Murdyantoro, and H. B. Widodo, "Histogram Equalization for Improving Quality of Low-Resolution Ultrasonography Images," *TELKOMNIKA Telecommunication Computing Electronics and Control,* vol. 15, no. 3, pp. 1397-1408, 2017.

[27] R. Supriyanti, A. R. Subhi, Y. Ramadhani, and H. B. Widodo, "Calculating Ventricle's Area based on Clinical Dementia Rating (CDR) Values on Coronal MRI image," *20th International Conference on Computer-Based Patient Records and Error Prevention (ICCPREP)*, 2018.

[28] R. Buckner, *et al.*, "A unified approach for morphometric and functional data analysis in young, old, and demented adults using automated atlas-based head size normalization: reliability and validation against manual measurement of total intracranial volume.," *Neuroimage*, vol. 23, pp. 724-738, 2004.
[29] E. Rubin, *et al.*, "A prospective study of cognitive function and onset of dementia in cognitively healthy elders.," *Arch Neurol*, vol. 55, pp. 395-401, 1998.
[30] Y. Zhang, M. Brady, and S. Smith, "Segmentation of brain MR images through a hidden Markov random field model and the expectation maximization algorithm," *IEEE Trans. Med. Imaging*, vol. 20, no. 1, pp. 45-57, 2001.
[31] A. Fotenos, A. Snyder, L. Girton, J. Morris, and R. Buckner, "Normative estimates of cross-sectional and longitudinal brain volume decline in aging and AD," *Neurology*, vol. 64, pp. 1032-1039, 2005.
[32] R. Supriyanti, *et al.*, "Active Contour Method for Identifying Area of Sagittal and Axial Slices to Identify the Severity of Alzheimer's disease," *International Conference on Recent Advances in Engineering and Technology (ICRAET)*, 2019.
[33] R. Supriyanti, A. R. Subhi, Y. Ramadhani, and H. B. Widodo, "Coronal slices segmentation of mri images using active contour method on initial identification of alzheimer severity level based on clinical dementia rating (CDR)," *J. Eng. Sci. Technol.*, vol. 14, no. 3, pp. 1672-1686, 2019.

BIOGRAPHIES OF AUTHORS

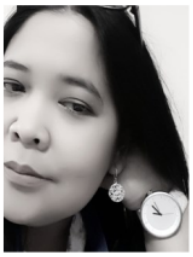

Retno Supriyanti is an academic staff at Electrical Engineering Department, Jenderal Soedirman University, Indonesia. She received her PhD in March 2010 from Nara Institute of Science and Technology Japan. Also, she received her M.S degree and Bachelor degree in 2001 and 1998, respectively, from Electrical Engineering Department, Gadjah Mada University Indonesia. Her research interests include image processing, computer vision, pattern recognition, biomedical application, e-health, tele-health and telemedicine

Anugerah Kevin Marchel received his Bachelor degree from Electrical Engineering Depratment, Jenderal Soedirman University Indonesia. His research interest Image Processing field

Yogi Ramadhani is an academic staff at Electrical Engineering Department, Jenderal Soedirman University, Indonesia. He received his MS Gadjah Mada Universirt Indonesia, and his Bachelor degree from Jenderal Soedirman University Indonesia. His research interest including Computer Network, Decision Support Syetem, Telemedicine and Medical imaging

Haris Budi Widodo is an academic staff at Public Health Department, Jenderal Soedirman University, Indonesia. He received his Ph.D from Airlangga University Indonesia. Also He received his M.S degree and bachelor degree from Gadjah Mada University Indonesia. His research interest including public health, e-health and telemedicine

paper 4

ORIGINALITY REPORT

16%	8%	10%	6%
SIMILARITY INDEX	INTERNET SOURCES	PUBLICATIONS	STUDENT PAPERS

MATCH ALL SOURCES (ONLY SELECTED SOURCE PRINTED)

2%

★ www.essaydale.com

Internet Source

Exclude quotes	Off	Exclude matches	Off
Exclude bibliography	On		